Mechatronics 19 (2009) 348–356

Contents lists available at ScienceDirect

Mechatronics

journal homepage: www.elsevier.com/locate/mechatronics

Flexible joints control: A minimum-time feed-forward technique

Luca Consolini, Oscar Gerelli *, Corrado Guarino Lo Bianco, Aurelio Piazzi

Dip. di Ing. dell'Informazione, University of Parma, viale G.P. Usberti 181/A, I-43100 Parma, Italy

ARTICLE INFO

Article history:
Received 30 April 2007
Accepted 15 October 2008

Keywords:
Minimum-time control
Flexible joints
Feed-forward control

ABSTRACT

The paper proposes a linear programming approach to the feed-forward minimum-time control of flexible joints. Taking into account both input and output constraints, the optimal bang–bang control is computed by discretizing a continuous-time joint model and by solving a sequence of linear programming feasibility problems. The resulting joint motion is a smooth rest-to-rest motion without oscillations. Theoretical analysis is presented and proof of convergence is given. Experimental results illustrate the proposed open-loop technique. Comparisons are made with inversion-based techniques.

1. Introduction

The problem of minimum-time position control for industrial manipulators is a well known and studied issue in robotics. Unfortunately, any minimum-time performance is usually achieved by maximizing the actuators dynamic efforts possibly leading to undesirable results in the case of standard feedback controllers. Indeed, due to saturations, the system behavior could be characterized by overshoots and oscillations. These effects are even more relevant for robotic manipulators showing a significant elastic coupling between joints, like those designed to share their workspace with human beings. In such cases the use of elastic joints increases the system safety by reducing the arm stiffness. In fact, as stated in [2], by decoupling the actuators inertia from the inertia of the links, it is possible to reduce the end-effector impact force such to limit potential danger to the operator. In recent literature a considerable attention has been given to the control of robot with flexible joints, see for instance [6,1,3], or [18] for a survey.

A major drawback of manipulators with a significant elastic coupling is that the output reacts slowly to the input, thus degrading the manipulator performances. Hence, it is interesting to consider the minimum-time control problem, that is to find the control input that allows performing a desired rest-to-rest transition for the end-effector, by minimizing at the same time the robot traveling time. This makes it possible to improve the resulting control performances despite the elastic coupling.

However, for such kind of robots, any sudden torque change, an implicit requirement of minimum-time motions, can excite the oscillatory dynamics. It is therefore important to introduce, together with the usual input constraints considered in the robotic literature, also output constraints. In this paper a time-optimal solution for an electrically driven flexible-joint arm is proposed. Explicit bounds on the motor feeding voltage are considered but, at the same time, a zero overshoot solution is required.

The minimum-time transition is obtained by discretizing the continuous-time model of the flexible joint and formulating an equivalent discrete-time optimization problem solved by means of linear programming techniques. More precisely, upper and lower bounds on the input voltage, as well as those on output overshoot and undershoot, are expressed by linear inequalities on a vector $\mathbf{u}$, representing the input voltages at sampling times. The optimization method searches the input vector $\mathbf{u}$ such that the end-effector performs a rest-to-rest transition in a number of steps less or equal than an initial guess n, while fulfilling the input and output constraints. Hence, the minimum-time problem is reformulated as a feasibility test for a linear programming (LP) problem and the minimum number of steps required to complete the given rest-to-rest transition can be found through a simple bisection algorithm. Since the sampling time T is fixed, minimizing the number of steps implies achieving the minimum-time solution which fulfills the given constraints.

The use of linear programming techniques for solving minimum-time problems for linear discrete-time systems, subject to bounded inputs, dates back to Zadeh [19]. Subsequently, many contributions have appeared focusing on various improvements. For example a faster algorithm is proposed in [5]. Work [11] presents a more general linear programming algorithm for solving optimal control problems for linear systems under generic constraints. In [10] a feasibility test is presented to improve the algorithm speed. For what concerns time-optimal control for continuous-time systems, a related result, under different hypotheses, is presented in [17]. It applies a comparison principle to a

* Corresponding author.
E-mail addresses: lucac@ce.unipr.it (L. Consolini), gerelli@ce.unipr.it (O. Gerelli), guarino@ce.unipr.it (C. Guarino Lo Bianco), piazzi@ce.unipr.it (A. Piazzi).

0957-4158/$ - see front matter © 2008 Elsevier Ltd. All rights reserved.
doi:10.1016/j.mechatronics.2008.10.005

time-optimal control problem for a class of state-constrained second-order systems.

The paper is organized as follows. In Section 2 the dynamic model of a flexible joint is devised. It will be used for the synthesis and the validation of the proposed control technique. In Section 3 the control problem is proposed and a solution is obtained in the subsequent section by means of a linear programming algorithm. An experimental test case is discussed in Section 5, while Section 6 draws the final conclusions.

Notation: Given a sequence $u(k) : \mathbb{Z} \to \mathbb{R}$, $U(z) = \mathscr{Z}\{u(k)\}$ represents its Z-transform, $\|u(k)\|_\infty = \max\{|u(k)| : k \in \mathbb{Z}\}$ is the infinity norm of $u(k)$. For $x \in \mathbb{R}$, $\lfloor x \rfloor = \max\{i \in \mathbb{Z} | i < x\}$ is the floor of x and $1_n \in \mathbb{R}^n = (1, 1, \ldots, 1)^T$. Given a matrix $\mathbf{M} \in \mathbb{R}^{n\times n}$, $\|\mathbf{M}\|_2 = \max\{\|Ax\| : x \in \mathbb{R}^n \text{ with } \|x\| = 1\}$ is the 2-norm.

2. Flexible-joint model

In this paper, the minimum-time control problem is solved for a single flexible-joint device produced by Quanser Consulting. Fig. 1 shows the top view of the considered system: a rigid arm is connected, through a flexible joint, to a rotating "body", which is actuated by a dc servo motor. Both the body and the arm can rotate around the vertical axis "O" of Fig. 1. The elastic coupling between the body and the arm is obtained by means of two springs whose stiffness is K_e and whose unstretched length is l_0.

The control technique proposed in Section 4 is based on the knowledge of the system model. For this reason, an accurate nonlinear model, mainly used for simulation purposes, is proposed in the following. The linearized version of the same model, to be used for the controller synthesis, is then devised.

Spring forces $\mathbf{f}_1$ and $\mathbf{f}_2$ cover an important role in the system dynamics. In order to evaluate their amplitude, let us assign a reference frame {1} whose origin is located in "O" and integral with the body. Moreover, let us assign a further frame {2}, located in "O" but integral with the arm, and indicate by θ_2 the joint angle between the two frames. Angle θ_2 is counterclockwise positive. In the same way, let us indicate by θ_1 the counterclockwise positive joint angle between the body frame {1} and a given stationary frame.

The three points "A", "B", and "C" shown in Fig. 1 can be described with respect to frame {1} by means of three vectors $\mathbf{p}_a := [-d_m\ h]^T$, $\mathbf{p}_b := [d_m\ h]^T$, and $\mathbf{p}_c := [-R\sin\theta_2\ R\cos\theta_2]^T$ where d_m, h, and R are the geometrical dimensions reported in the same figure.

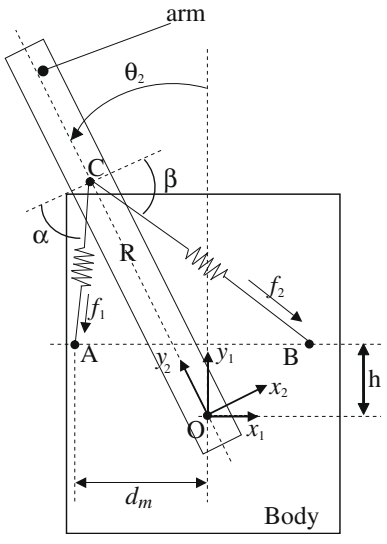

Fig. 1. Flexible-joint experiment: top view.

The spring force norms, i.e., $f_1 := \|\mathbf{f}_1\|$ and $f_2 := \|\mathbf{f}_2\|$, depend on the spring lengths l_1 and l_2 according to equations

$$f_1 = K_e(l_1 - l_0), \tag{1}$$
$$f_2 = K_e(l_2 - l_0), \tag{2}$$

where l_1 and l_2 can be evaluated as follows:

$$l_1 = \|\mathbf{p}_c - \mathbf{p}_a\| = \sqrt{R^2 + d_m^2 + h^2 - 2R(d_m \sin\theta_2 + h\cos\theta_2)}, \tag{3}$$
$$l_2 = \|\mathbf{p}_c - \mathbf{p}_b\| = \sqrt{R^2 + d_m^2 + h^2 + 2R(d_m \sin\theta_2 - h\cos\theta_2)}. \tag{4}$$

Forces acting on point "C" can be described with respect to frame {2} leading to

$$\begin{bmatrix} f_{1_x} \\ f_{1_y} \end{bmatrix} = \begin{bmatrix} f_1\cos(\alpha) \\ f_1\sin(\alpha) \end{bmatrix} = \begin{bmatrix} -K_e(l_1 - l_0)\cos(\alpha) \\ -K_e(l_1 - l_0)\sin(\alpha) \end{bmatrix}$$

and

$$\begin{bmatrix} f_{2_x} \\ f_{2_y} \end{bmatrix} = \begin{bmatrix} f_2\cos(\beta) \\ f_2\sin(\beta) \end{bmatrix} = \begin{bmatrix} K_e(l_2 - l_0)\cos(\beta) \\ -K_e(l_2 - l_0)\sin(\beta) \end{bmatrix},$$

where $\alpha, \beta \in \mathbb{R}^+$ are the two auxiliary angles shown in Fig. 1 which can be evaluated by means of the following equations:

$$\alpha(\theta_2) = \arctan\left[\frac{R\cos(\theta_2) - h}{d_m - R\sin(\theta_2)}\right] - \theta_2,$$
$$\beta(\theta_2) = \arctan\left[\frac{R\cos(\theta_2) - h}{d_m + R\sin(\theta_2)}\right] + \theta_2.$$

Elastic forces induce an elastic nonlinear torque in the arm that can be expressed as

$$\tau_e(\theta_2) = [-f_{1_x}(\theta_2) - f_{2_x}(\theta_2)]R. \tag{5}$$

It is worth noting that components f_{1_y} and f_{2_y} do not generate any torque with respect to "O".

It is now possible to propose the dynamic equation of the rigid arm described with respect to "O"

$$J_{load}(\ddot{\theta}_2 + \ddot{\theta}_1) = [-f_{1_x}(\theta_2) - f_{2_x}(\theta_2)]R - B_{eq}^L\dot{\theta}_2, \tag{6}$$

where J_{load} is the arm inertia evaluated with respect to "O", while B_{eq}^L is the friction coefficient associated to angular velocity $\dot{\theta}_2$. Practically, arm dynamics takes into account torques which are due to inertia, friction and elasticity.

It is similarly possible to devise the dynamic equation of the "body". It is made of a chain of inertial loads and reduction gears driven by a permanent magnet dc motor according to the scheme shown in Fig. 2. More precisely, the motor, characterized by an inertia J_m, is connected through a chain of reduction gears to the output shaft. Each reduction gear is characterized by a reduction ratio, see, e.g. k_G, k_I, and an inertia, see, e.g. J_{120}, J_{72}, and J_{24}. The first reduction gear is characterized by an efficiency coefficient η_G, while the body inertia is J_{FJ}. Output angle θ_1 is measured through a potentiometer coupled to the output shaft by means of a gear which has reduction ratio $k = 1$.

The system is affected by torques which are due to inertia, friction and elasticity, yielding to

$$J_{eq}^0\ddot{\theta}_1 = \tau^0 - B_{eq}^0\dot{\theta}_1 - [-f_{1_x}(\theta_2) - f_{2_x}(\theta_2)]R + B_{eq}^L\dot{\theta}_2, \tag{7}$$

where J_{eq}^0 is the equivalent inertia of the system composed by motor, reduction gears, and "body", τ^0 is the motor torque reflected through the gears ratios, while B_{eq}^0 is the friction coefficient associated to angular velocity $\dot{\theta}_1$. All quantities in (7) are referred to the output shaft of the system. For the system of Fig. 2 the equivalent inertia can be expressed as

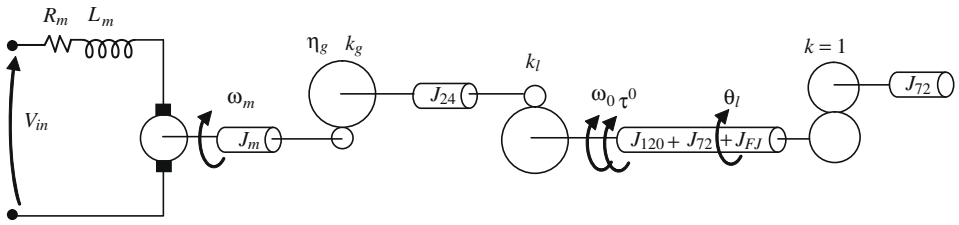

Fig. 2. Inertia and gears ratio chain view from motor rotor axis.

$$J_{eq}^0 = \left[J_m k_g^2 k_l^2 \eta_g + J_{24} k_l^2 + J_{120} + 2J_{72} + J_{FJ}\right].$$

The dynamics of a dc motor is given by the following equations [8]:

$$\begin{cases} L\frac{di}{dt} = -R_m i - k_m \omega_m + v_{in}; \\ \tau_m = k_m i, \end{cases} \tag{8}$$

where τ_m is the torque at the output shaft of the dc motor, L_m is the armature inductance, ω_m is the motor angular velocity, k_m is the motor electric constant, R_m is the motor winding resistance, and v_{in} is the motor feeding voltage.

Due to (8), the motor electrical pole is equal to

$$\frac{R_m}{L_m} \simeq 1 \cdot 10^4 \text{ rad s}^{-1},$$

which is negligible with respect to the mechanical pole equal to 11 rad s^{-1}. Therefore (8) can be approximated as follows:

$$\tau_m \simeq k_m \left(\frac{v_{in} - k_m \omega_m}{R_m}\right).$$

Hence, according to Fig. 2, the output torque τ^0 can be expressed as

$$\tau^0 = \tau_m (k_g k_l \eta_g \eta_m) = \frac{k_g k_l k_m \eta_g \eta_m}{R_m} v_{in} - \frac{k_g^2 k_l^2 k_m^2 \eta_g \eta_m}{R_m} \dot{\theta}_1, \tag{9}$$

where η_m is the motor efficiency.

Bearing in mind (9), (7) can be rewritten as follows:

$$J_{eq}^0 \ddot{\theta}_1 = -G\dot{\theta}_1 + B_{eq}^L \dot{\theta}_2 - [-f_{1_x}(\theta_2) - f_{2_x}(\theta_2)]R + H v_{in}, \tag{10}$$

where

$$G = \frac{k_g^2 k_l^2 k_m^2 \eta_g \eta_m}{R_m} + \beta_{eq}^0, \tag{11}$$

$$H = \frac{k_g k_l k_m \eta_g \eta_m}{R_m}. \tag{12}$$

Eqs. (6) and (10) represent the complete nonlinear dynamic model of the flexible joint and are used to simulate the system behavior. For the synthesis of the control technique proposed in Section 4, an equivalent linear model is devised. Elastic torque τ_e is the sole nonlinear term which appears in (6) and (10). It can be linearized in $\theta_2 = 0$ leading to $\tau_e \simeq -K_{stiff}\theta_2$, where

$$K_{stiff} = -\left.\frac{d\tau_e(\theta_2)}{d\theta_2}\right|_{\theta_2=0} = \frac{2R^2 d_m^2 k_l}{(R-h)^2 + d_m^2}$$

is the stiffness constant. Consequently, (6) and (10) can be rewritten as

$$J_{eq}^0 \ddot{\theta}_1 = -G\dot{\theta}_1 + B_{eq}^L \dot{\theta}_2 + K_{stiff}\theta_2 + H v_{in}, \tag{13}$$

$$J_{load}(\ddot{\theta}_2 + \ddot{\theta}_1) = -B_{eq}^L \dot{\theta}_2 - K_{stiff}\theta_2. \tag{14}$$

The output of the system is given by the angle formed by the end-effector with respect to the stationary frame. Hence, $y = \theta_1 + \theta_2$, i.e, the sum of the angle between the body and the stationary frame and the angle formed by the arm with respect to the body. Finally, it is possible to rewrite (13) and (14), into a state-space form

$$\begin{cases} \dot{\mathbf{x}} = \mathbf{A}\mathbf{x} + \mathbf{b} v_{in}, \\ \mathbf{y} = \mathbf{C}\mathbf{x} + \mathbf{d} v_{in}, \end{cases}$$

by assuming $\mathbf{x} := [x_1 x_2 x_3 x_4]^T = [\theta_1 \theta_2 \dot{\theta}_1 \dot{\theta}_2]^T$ and defining

$$\mathbf{A} := \begin{bmatrix} 0 & 0 & 1 & 0 \\ 0 & 0 & 0 & 1 \\ 0 & \frac{K_{stiff}}{J_{eq}^0} & -\frac{G}{J_{eq}^0} & \frac{B_{eq}^L}{J_{eq}^0} \\ 0 & -\frac{K_{stiff}(J_{load}+J_{eq}^0)}{J_{load}J_{eq}^0} & \frac{G}{J_{eq}^0} & -\frac{B_{eq}^L(J_{load}+J_{eq}^0)}{J_{load}J_{eq}^0} \end{bmatrix}, \quad \mathbf{b} := \begin{bmatrix} 0 \\ 0 \\ \frac{H}{J_{eq}^0} \\ -\frac{H}{J_{eq}^0} \end{bmatrix},$$

$$\mathbf{C} := [1 \quad 1 \quad 0 \quad 0], \quad \mathbf{d} := 0. \tag{15}$$

The corresponding discrete-time system is obtained from (15) by the zero-order hold equivalence, yielding to

$$\begin{cases} \dot{\mathbf{x}}_{n+1} = \mathbf{A}_0 \mathbf{x}_n + \mathbf{b}_0 v_{in}, \\ \mathbf{y}_{n+1} = \mathbf{C}_0 \mathbf{x}_{n+1} + \mathbf{d}_0 v_{in}, \end{cases} \tag{16}$$

where $\mathbf{A}_0 = e^{AT}$, $\mathbf{b}_0 = \int_0^T e^{A\tau}\mathbf{b}\,d\tau$, $\mathbf{C}_0 = \mathbf{C}$, $\mathbf{d}_0 = \mathbf{d}$ and T is the sampling period.

3. Problem formulation

In this section, the minimum-time feed-forward control problem is stated for scalar discrete-time systems in a general case and then for the specific case of the flexible joint presented in Section 2.

3.1. General formulation

A linear discrete-time system Σ_d is described by the proper scalar transfer function

$$H(z) = \frac{b(z)}{a(z)} = \frac{b_m z^m + b_{m-1} z^{m-1} + \cdots + b_0}{a_n z^n + a_{n-1} z^{n-1} + \cdots + a_0}. \tag{17}$$

$a(z)$, $b(z)$ are coprime, Σ_d is stable, and its static gain $H(1) \neq 0$. The system input and output sequences are denoted by $u(k)$ and $y(k)$, respectively, $k \in \mathbb{Z}$.

The behavior $\mathscr{B}_d$ of system Σ_d is the set of all input–output pairs $(u(\cdot), y(\cdot))$, where $u(\cdot), y(\cdot) : \mathbb{Z} \to \mathbb{R}$, satisfying the difference equation

$$\begin{aligned} &a_n y(k+n) + a_{n-1} y(k+n-1) + \cdots + a_0 y(k) \\ &\quad = b_m u(k+m) + b_{m-1} u(k+m-1) + \cdots + b_0 u(k). \end{aligned} \tag{18}$$

The set of input–output equilibrium points of Σ_d is $\mathscr{E} := \{(u, y) \in \mathbb{R}^2 : y = H(1)u\}$ and the set $\mathscr{K}_s \subset \mathscr{B}_d$ of all rest-to-rest constrained transitions from $(0,0) \in \mathscr{E}$ to $(\frac{y_f}{H(1)}, y_f) \in \mathscr{E}$ is defined as follows.

Definition 1. Given the parameter set $\mathbf{s} := \{U_c, Y_c, y_f\}$, where $U_c := [u_c^-, u_c^+]$ and $Y_c := [y_c^-, y_c^+]$ are the constraint intervals for the input and output, respectively, and y_f is the final rest value of the output, $\mathscr{K}_\mathbf{s}$ is the set of all pairs $(u(\cdot), y(\cdot)) \in \mathscr{B}_d$ for which there exists $k_f \in \mathbb{N}$ such that

$$u(k) = 0 \ \forall k < 0, \quad u(k) = \frac{y_f}{H(1)} \ \forall k \geqslant k_f, \tag{19}$$

$$u(k) \in U_c \quad \forall k \in \mathbb{Z}, \tag{20}$$

$$y(k) = 0 \ \forall k < 0, \quad y(k) = y_f \ \forall k \geqslant k_f, \tag{21}$$

$$y(k) \in Y_c \quad \forall k \in \mathbb{Z}. \tag{22}$$

The minimum-time feed-forward constrained control problem for discrete-time systems consists in finding the optimal input sequence $u^*(k)$, $k = 0, 1, \ldots, k_f^* - 1$ for which the pair $(u^*(\cdot), y^*(\cdot)) \in \mathscr{K}_{\mathbf{s}}$ is a minimizer for the optimization problem

$$k_f^* = \min_{(u(\cdot),y(\cdot))\in\mathscr{K}_{\mathbf{s}}} K_f(u(\cdot), y(\cdot)), \tag{23}$$

where

$$K_f(u(\cdot), y(\cdot)) := \min\left\{k_1 \in \mathbb{N} : u(k) = \frac{y_f}{H(1)},\ y(k) = y_f \ \forall k \geqslant k_1\right\}$$

is the rest-to-rest transition time associated to pair $(u(\cdot),y(\cdot))$.

3.2. An approximated solution to the continuous-time problem using discretization

Given a continuous system $H(s)$, a time-optimal constrained control problem can be converted into the previously defined discrete-time one through the following procedure:

- find the discretized system $H(z)$ using a zero-order equivalence, with sampling period T, by applying relation $H(z) = (1 - z^{-1})\mathscr{Z}\{\frac{H(s)}{s}\}$;
- find the time-optimal input sequence $u^*(k)$ such that (23) is satisfied;
- transform the discrete sequence $u^*(k)$ into the continuous function $u_c(t)$ by using a zero-order hold, that is the signal is kept constant between one sampling time and the next one;
- apply the input function $u_c(t)$ to the continuous-time system.

Fig. 3 gives a representation of the signals involved in the discretization. Due to the procedure given before, the control found with this method is optimal only with respect to the class of input functions which are constant in each sampling period. Hence, the resulting transition time is higher than the minimum one achievable with continuous-time input functions.

Moreover note that $y^*(k)$ fulfills for certainty the prescribed constraints, so that the output $y_c(t)$ of the continuous system satisfies the following condition:

$$y_c(kT) \in Y_c \quad \forall k \in \mathbb{Z},$$

while it is not guaranteed that $y_c(t) \in Y_c$ if the time t is not multiple of the sampling period T. In other word, the output may exceed the prescribed bounds between two consecutive sampling times. Obviously, the maximum constraints violation of $y_c(t)$ is strictly related to the choice of the sampling period T. In Section 4.1 a bound on maximum violation is found and, in turn, considerations on the choice of T are presented.

3.3. Problem formulation for the flexible-joint system

Consider the system obtained by discretizing the rotary flexible-joint system introduced in Section 2. The problem to be solved is the following one.

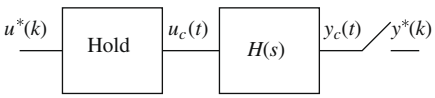

Fig. 3. Zero-order hold equivalence.

Problem 1 (*Minimum-time control problem for the flexible joint*). Consider the discrete-time system (16) and intervals $U_c := [u_c^-, u_c^+]$ of admissible values for the input voltage v_{in} and $Y_c := [y_c^-, y_c^+]$ of admissible values for the output angle $y = \theta_1 + \theta_2$, where y_c^- and y_c^+ represent maximum undershoot and overshoot specifications. Find the input sequence $u^*(k)$ that minimizes the time required for the rest-to-rest transition of the output $y^*(k)$ from the initial angle 0 to the desired final angle y_f, while satisfying the input and output constraints

$$u^*(k) \in U_c, y^*(k) \in Y_c \quad \forall k > 0.$$

4. Problem resolution

In this section a general method is proposed for the solution of the rest-to-rest control problem for scalar systems with bounded input and output. In the next section it will be applied to the linearized flexible-joint system.

The following theorem proposes a feasibility condition for the existence of a solution of the constrained rest-to-rest transition problem, which is equivalent to the non-emptiness of set $\mathscr{K}_{\mathbf{s}}$ defined in Definition 1.

Theorem 1. *Set $\mathscr{K}_{\mathbf{s}}$ is not empty if*

$$\left\{0, \frac{y_f}{H(1)}\right\} \subset (u_c^-, u_c^+) \quad \text{and} \quad \{0, y_f\} \subset (Y_c^-, Y_c^+) \tag{24}$$

with the convention that $\frac{y_f}{H(1)} = 0$ if $H(s)$ has a pole in 1.

Proof 1. See Appendix A. □

The following proposition allows to convert the time-optimal problem into a LP problem.

Proposition 1. *The set $\mathscr{K}_{\mathbf{s}}$ of all rest-to-rest constrained transitions is not empty if and only if there exist $k_f \in \mathbb{N}$ and a vector $\mathbf{u} \in \mathbb{R}^{k_f}$ for which the following LP problem is feasible:*

$$y_c^- \cdot \mathbf{1}_{k_f} \leqslant \mathbf{H}\mathbf{u} \leqslant y_c^+ \cdot \mathbf{1}_{k_f}, \tag{25}$$

$$u_c^- \cdot \mathbf{1}_{k_f} \leqslant \mathbf{u} \leqslant u_c^+ \cdot \mathbf{1}_{k_f}, \tag{26}$$

$$\bar{\mathbf{H}}\begin{bmatrix}\mathbf{u} \\ \frac{y_f}{H(1)} \cdot \mathbf{1}_n\end{bmatrix} = y_f \cdot \mathbf{1}_n, \tag{27}$$

where $\mathbf{H} \in \mathbb{R}^{k_f \times k_f} = (h_{i,j})$ is defined by $h_{i,j} := h(i-j)$ and $\bar{\mathbf{H}} \in \mathbb{R}^{n \times (k_f+n)} = \bar{h}(i,j)$ by $\bar{h}_{i,j} := h(i + k_f - j)$.

Proof 2. (Necessity) Assume that there exists a vector $\mathbf{u}$ for which Eqs. (25)–(27) are satisfied. Define the input sequence

$$u(k) = \begin{cases} 0 \text{ if } k < 0, \\ \mathbf{u}(k) \text{ if } 0 \leqslant k < k_f, \\ \frac{y_f}{H(1)} \text{ if } k \geqslant k_f, \end{cases} \tag{28}$$

which satisfies properties (19) and (20) of Definition 1. The output is given by $y(k) = \sum_{i=0}^{\infty} u(k-i)h(i)$, where $h(k)$ is the impulse response of the discrete system. Setting $\mathbf{y} \in \mathbb{R}^{k_f} = (y_1, y_2, \ldots, y_{k_f})^T : y_i = y(i)$ and $\bar{\mathbf{y}} \in \mathbb{R}^n : \bar{y}_i = y(k_f + i)$, it is

$$\mathbf{y} = \mathbf{H}\mathbf{u}, \bar{\mathbf{y}} = \bar{\mathbf{H}}\begin{bmatrix}\mathbf{u} \\ \frac{y_f}{H(1)} \cdot \mathbf{1}_n\end{bmatrix}$$

and, by virtue of (25), $y(k)$ satisfies property (22) of Definition 1, $\forall k < k_f$. Finally $y(k) = y_f, \forall k \geqslant k_f$ because of Lemma 1 (see Appendix A).

(Sufficiency) Assume that for a given k_f, the set $\mathscr{K}_{\mathbf{s}}$ is not empty, therefore it contains at least a pair $(u(k),y(k))$. If $\mathbf{u}$ and $\mathbf{y}$ are defined as above, due to (20) and (22) it follows that

$$u_c^- \cdot \mathbf{1}_{k_f} < \bar{u} < u_c^+ \cdot \mathbf{1}_{k_f},$$
$$y_c^- \cdot \mathbf{1}_{k_f} < \bar{y} < y_c^+ \cdot \mathbf{1}_{k_f},$$

moreover, being $y(k) = \sum_{i=0}^{+\infty} h(k-i)u(i)$,

$$\begin{bmatrix} \mathbf{y} \\ \bar{\mathbf{y}} \end{bmatrix} = \left[\begin{array}{c|c} \mathbf{H} & 0 \\ \hline \bar{\mathbf{H}} & \end{array}\right] = \begin{bmatrix} \bar{u} \\ \frac{y_f}{H(1)} \cdot \mathbf{1}_n \end{bmatrix},$$

therefore Eqs. (25)–(27) are satisfied. □

By virtue of Proposition 1, the minimum-time k_f^* and an associated optimal feed-forward input $u^*(k)$, $k = 0, 1, \ldots k_f^* - 1$ can be determined by means of a sequence of LP feasibility tests, defined by (25)–(27), through the simple bisection algorithm reported below. In this algorithm $LPP(\mathbf{s}, H(z), k_f, \mathbf{u})$ denotes a linear programming procedure that solves problem (25)–(27): if the problem is feasible it returns a Boolean true value along with a solution $\mathbf{u}$. Note that parameter set $\mathbf{s} := \{U_c, Y_c, y_f\}$ (see Definition 1) contains the input and output constraints and the desired final output value.

Algorithm 1

Compute the minimum-time feed-forward control with input and output constraints for discrete-time systems
input $H(z)$ and $\mathbf{s}$
output k_f^* and $u^*(k)$, $k = 0, 1, \ldots, k_f^* - 1$
begin
  $k_f \leftarrow 1$;
  $l \leftarrow 0$;
  while $\sim LPP(\mathbf{s}, H(z), k_f, \mathbf{u})$ **do**
    $l \leftarrow k_f$;
    $k_f \leftarrow 2k_f$
  end
  $h \leftarrow k_f$;
  while $h - l > 1$ **do**
    $k_f \leftarrow \lfloor \frac{h+l}{2} \rfloor$
    If $\sim LPP(\mathbf{s}, k_f, \mathbf{u})$ **then**
      $l \leftarrow k_f$;
    else
      $h \leftarrow k_f$
    end
  end
  $k_f^* \leftarrow h$;
  $u^*(k) \leftarrow \mathbf{u}$
end

4.1. Choice of the sampling period

The choice of sampling period T is critical for the proposed algorithm, since larger values of T allow a faster computation but less accurate results.

The continuous-time input signal $u_c(t)$ is obtained, from the optimal discrete-time sequence $u^*(k)$, through a zero-order hold, that is the signal is kept constant between one sampling time and the next one

$$u_c(t) = u^*(k), \quad \text{where } k = \{\max i | iT \leqslant t\}.$$

Let $y_c(t)$ be the system output and $y^*(k)$ the corresponding sampled signal. The proposed approach guarantees that $y^*(k)$ satisfies the prescribed constraints, that is

$$y_c(kT) \in Y_c \quad \forall k \in \mathbb{Z}.$$

It is worth noting that there is not any certainty that $y_c(t) \in Y_c$ for $t \neq kT$, since the optimization algorithm only checks the constraints at the sampling times. The following proposition shows that the maximum excursion of the continuous-time signal $y_c(t)$ from the prescribed constraints is bounded by a term that goes to 0 as the sampling time T approaches to 0.

Proposition 2. *Consider the continuous-time scalar system*

$$\dot{x} = \mathbf{A}x + \mathbf{b}u, y = \mathbf{C}x,$$

where A is a nonsingular matrix and let $Y_c := [y_c^-, y_c^+]$ *be two nonempty intervals. If u(t) is constant in [kT,(k + 1)T[* $\forall k \in \mathbb{Z}$, *and* $y(kT) \in Y_c$ $\forall$ *t = k T, then for any integer* $l \in \mathbb{Z}$, $l \geqslant 2$ *the following inequality is satisfied:*

$$\begin{aligned} &\max_{t\in\mathbb{R}} \{y(t) - y_c^+, y_c^- - y(t)\} \\ &\leqslant \left(\|C\|(e^{\|A\|T} - 1 - \|A\|T) - \sum_{i=2}^{l} \frac{T^i}{i!} \|C\| \|A\|^i - \|CA^i\| \right) \\ &\cdot (\max_k \|x(kT)\| + \|B\| \|A\|^{-1} \max_k \|u(kT)\|). \end{aligned} \tag{29}$$

Proof 3. See Appendix B. □

Remark 1. Proposition 2 gives a set of estimates for the maximum output constraints violation $\max_{t\in\mathbb{R}}\{y(t) - y_c^+, y_c^- - y(t)\}$. The estimates depend on the integer parameter l and become more accurate as l increases and the sample time T decreases.

Note that the proposed approach guarantees the discretized system reaches the desired equilibrium at the final sample k_f^*, but this does not necessarily imply that also the underlying continuous-time system reaches the equilibrium. The following proposition shows that this requirement is fulfilled if a restriction on sampling time T is imposed.

Proposition 3. *Let be given a continuous-time system* Σ *with transfer function*

$$H(s) = \frac{b_m s^m + b_{m-1} s^{m-1} + \cdots + b_0}{s^n + a_{n-1} s^{n-1} + \cdots + a_0},$$

where $n > m$, $T > 0$, $t_0 \in \mathbb{R}$. *Consider an input–output pair* $(u(t), y(t)) \in \mathscr{B}$ *such that*

$$\begin{aligned} &u(t) = \frac{y_f}{H(0)} \quad \forall t \geqslant t_0, \\ &y(t_0 + kT) = y_f \quad \text{for } k = 0, \ldots, n-1, \end{aligned} \tag{30}$$

and for which the distinct roots $p_1, \ldots, p_l$ *of the characteristic polynomial* $s^n + a_{n-1} s^{n-1} + \cdots + a_0$ *satisfy*

$$p_i - p_r \neq k\frac{2\pi j}{T} \quad \forall i, r = 1, \ldots, l, \ \forall k \in \mathbb{Z} - \{0\}, \tag{31}$$

then the following condition is satisfied:

$$y(t) = y_f \quad \forall t \geqslant t_0.$$

Proof 4. See Appendix C. □

Remark 2. Condition (31) is satisfied if

$$T < \frac{2\pi j}{\max_i \{\mathrm{Im}\{p_i\}\}} \quad \forall i = 1, \ldots, l, \tag{32}$$

that is the sampling time is less that 2π divided by the largest imaginary part among the system poles.

In conclusions the sampling time T must be chosen sufficiently small such that condition (32) is satisfied and bound (29) is sufficiently small.

5. Simulation and experimental results

In this section the control method proposed in Section 4 is applied to the case of the flexible joint model derived in Section 2.

Simulation are executed on a P4 3.0 GHz computer within Matlab programming environment. The freely available library GPLK (GNU Linear Programming Kit) [4] is used as linear programming solver and interfaced with Matlab through [12]. Experimental results are obtained by interfacing the flexible-joint device with Matlab through the Quanser Q4 PCI data acquisition board.

By substituting the flexible-joint parameters defined in Table 1 in state-space model (15), the following numerical representation for the plant is obtained:

$$\mathbf{A} := \begin{bmatrix} 0 & 0 & 1 & 0 \\ 0 & 0 & 0 & 1 \\ 0 & 379.9 & -56.65 & 2.956 \\ 0 & -512.9 & 56.65 & -3.99 \end{bmatrix}, \quad \mathbf{b} := \begin{bmatrix} 0 \\ 0 \\ 93.74 \\ -93.74 \end{bmatrix}$$

$$\mathbf{C} := [1 \quad 1 \quad 0 \quad 0], \quad \mathbf{d} := 0. \tag{33}$$

Two different cases have been considered. In the first one, output constraints have been imposed only on the end-effector angle. According to the flexible-joint model in Section 2, this imply to set a limit on the sum of the rotation angle of the body, θ_1, plus the displacement θ_2 induced by the joint elasticity, i.e. $y = \theta_1 + \theta_2$. In the second case, additional constraints on the joint displacement θ_2 have been added. In fact, limiting the angle induced by the joint flexibility between the arm and the rotating body, allows keep bounded the torsion moment on the joint itself, which in turn, implies reducing the reflected joint solicitation torque.

5.1. Control without constraints on θ_2

A rest-to-rest transition from $y = 0$ to $y = y_f = \pi/4$ is considered. The flexible joint is driven with an amplifier whose maximum bipolar voltage is equal to ±5 V. Therefore, the input constraint is $\|u(t)\|_\infty \leqslant 5$, so that $U_c = [-5,+5]$. A strong requirement has been set on the output function: a maximum of 0.1% overshoot and undershoot is allowed on y, so that $Y_c = [-7.8539 \cdot 10^{-4}, \pi/4 + 7.8539 \cdot 10^{-4}]$. First of all note that condition (24) of Theorem 1 is satisfied. In fact, since the flexible joint discretized transfer function has two poles in $z = 1$, condition (24) reduces to

$$\{0\} \in U_c, \quad \frac{\pi}{4} \in Y_c.$$

This mean that set $\mathscr{K}_\mathbf{s}$ is nonempty.

Condition (32) must be satisfied in order to ensure that the continuous-time system reaches the equilibrium with the same transient time of the discretized one. This implies that $T < 0.57$ s. In all the simulation examples, the sampling time has been chosen equal to $T = 0.001$ s. Simulation results, obtained with the algorithm described in Section 4, are shown in Figs. 4 and 5.

Fig. 4 highlights the bang–bang control input which makes it possible to obtain a rest-to-rest transition time of $t_f^* = 0.305$ s. Fig. 5 plots a comparison between the ideal simulated output and the real behavior of the flexible joint. The real output shows a small overshoot and undershoot: this is due to the small mismatching between the real plant and the flexible joint model devised in Section 2.

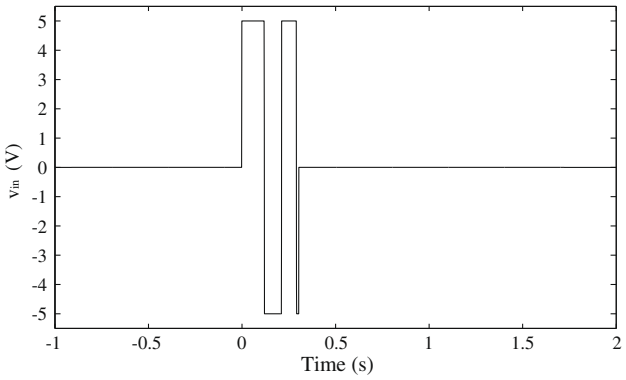

Fig. 4. Optimal input signal devised with the proposed approach.

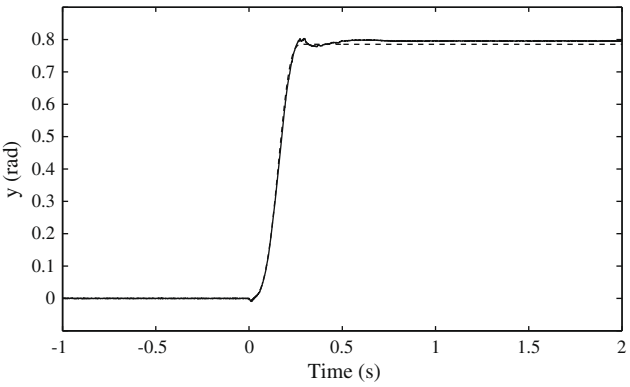

Fig. 5. Expected system output y (dashed line) and measured plant output (solid line).

The maximum error on the output constraints for the continuous-time system, obtained with (29) for a sampling time $T = 0.001$ s, is given by $\max_{t\in\mathbb{R}}\{y(t) - y_c^+, y_c^- - y(t)\} \leqslant 0.00113$ rad.

The herein proposed approach has been compared with that presented in [15,7], where a time-optimal control is found by means of dynamic inversion based on the so called "transition polynomials" (see [15]).

Results obtained by applying that planning method are shown in Figs. 6 and 7. Comparing Figs. 6 and 4, it is clearly visible that the approach based on "transition polynomials" allows to generate smoother input control. However, the output function presents a slightly oscillatory behavior, causing an increase of the real transition time with respect to the simulated one, which was equal to $t_f^* = 0.360$ s. Hence, the two methods are both suitable for the constrained control of the considered flexible joint. However, when the application requires rapid maneuvers, the proposed bang–bang control allows to perform the required output transition in a smaller time.

Table 1
Flexible-joint parameters.

Electrical data			Gears parameters			Viscous frictions	
R_m (Ω)	k_m (Nm/A)	η_m	k_g	k_l	η_g	B_{eq}^0 (N/s)	B_{eq}^L (N/s)
2.6	7.67×10^{-3}	0.69	14	5	0.9	14.99×10^{-3}	11.42×10^{-3}

J_m	J_{120}	J_{72}	J_{24}	J_{FJ}	J_{load}
Inertial parameters (kgm^2)					
0.386×10^{-6}	0.440×10^{-6}	5.274×10^{-6}	0.195×10^{-6}	2.10×10^{-3}	11.03×10^{-3}

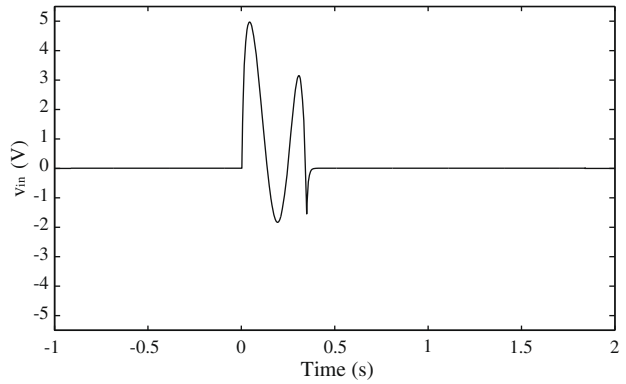

Fig. 6. Optimal transition polynomial input signal.

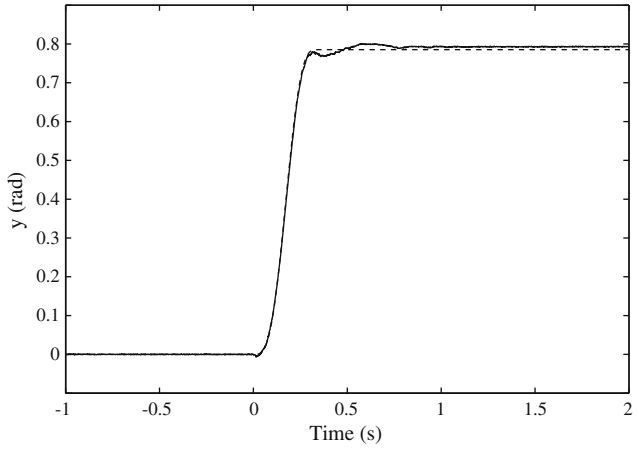

Fig. 7. Expected system output y (dashed line) and measured plant output (solid line).

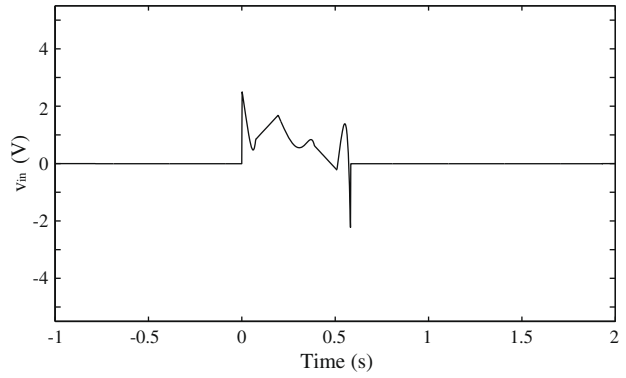

Fig. 8. The time-optimal control with angle limit on θ_2.

5.2. Control with constraints on θ_2

The minimum-time control law used in the previous simulations and experiments does not take care of the solicitation torque induced to the joint by the deflection angle θ_2: the only constraint that has been imposed is related to the end-effector position, i.e. the sum of $\theta_1 + \theta_2$.

On a real flexible-joint robot it can be interesting to devise a time-optimal transition control also constraining the maximum admissible displacement between the link position and the joint position, thus reducing the mechanical solicitation on the joint itself.

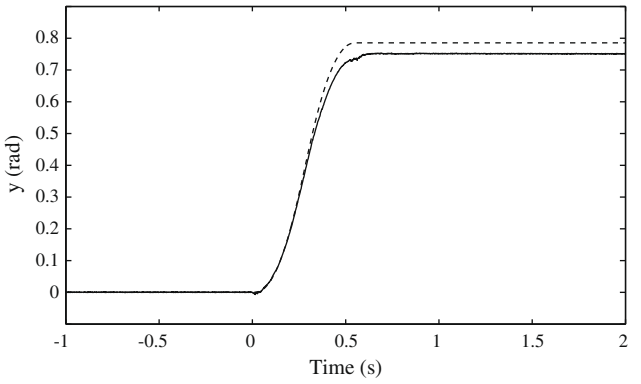

Fig. 9. Expected system output y (dashed line) and measured plant output (solid line).

Thus, under the same constraints used in previous section, a limit on θ_2 angle has been added such that $\theta_2 \in [-5\pi/180, 5\pi/180]$.

Simulated and experimental results are reported in Figs. 8 and 9. In particular in Fig. 10 is reported the time-waveform of the relative displacement between the arm and the rotating body. As it is shown, the θ_2 angle is constantly saturated to the imposed constraint value, and this is the reason why the optimal control is no longer a bang–bang function. Clearly the optimal transition time increases: in this case $t_f^* = 0.59$ s.

5.3. Computational complexity

In this section, some considerations are given for what concern the computational complexity of the time-optimal algorithm. In particular, Table 2 shows the computational time required by the proposed approach to devise the time-optimal control sequence. Symbol $\Delta\theta$ has been used to represent the overall rest-to-rest transition, while T indicates, as always, the sample time required by the discretization phase. As it can be seen, performances strongly

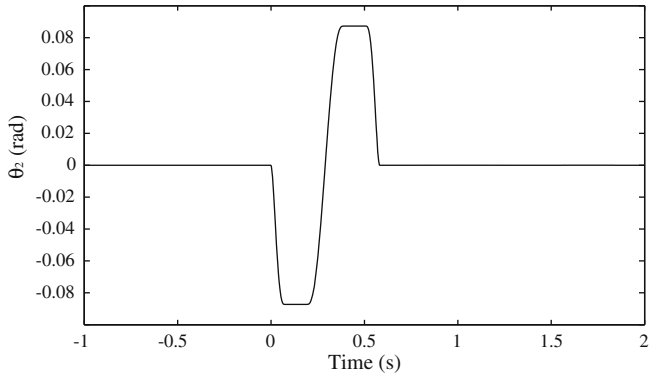

Fig. 10. θ_2 angle.

Table 2
Algorithm performances.

$\Delta\theta$ (rad)	T (s)	Computation time (s)	Transition time t_f^* (s)
$\pi/4$	$1 \cdot 10^{-3}$	$7.943 \cdot 10^{0}$	$3.05 \cdot 10^{-1}$
	$1 \cdot 10^{-2}$	$1.023 \cdot 10^{0}$	$3.10 \cdot 10^{-1}$
	$5 \cdot 10^{-2}$	$6.854 \cdot 10^{-1}$	$4.00 \cdot 10^{-1}$
$\pi/2$	$1 \cdot 10^{-3}$	$9.275 \cdot 10^{0}$	$3.88 \cdot 10^{-1}$
	$1 \cdot 10^{-2}$	$6.882 \cdot 10^{-1}$	$3.90 \cdot 10^{-1}$
	$5 \cdot 10^{-2}$	$8.906 \cdot 10^{-1}$	$5.00 \cdot 10^{-1}$

depend on the used sampling time: by reducing T, which means sampling the continuous-time system with an higher frequency, the dimension of the resulting LP problem increases, thus causing an increment of the total computational time. Considering the computational complexity, Karmarkar has shown in [13] that a linear programming problem can be solved by means of an algorithm with running time proportional to $n^{3.5}$, where n is the number of inequalities. In our case this would means that each feasibility test would require a time proportional to $n_s^{3.5}$, where n_s is the total number of samples. The complexity of the bisection search, with respect to the minimum number of samples, is given by $O(\log n_s)$, therefore the total complexity of the proposed algorithm is given by $O(\log n_s n_s^{3.5})$. In our tests the dual simplex method has been used. It is well known (see [16]) that the simplex method complexity is theoretically exponential with respect to n, due to the existence of special worst cases, but, in practice, the complexity is almost linear with respect to n. This would mean that the "practical" complexity of the proposed algorithm is $O(\log n_s n_s)$. In any case, it is important to keep the number of samples (which is inversely proportional to the sampling time T) as small as possible.

Generally the time required by the algorithm to obtain the optimal control has an order of magnitude of a few seconds and can be further improved if the algorithm is directly coded in C/C++. Since the Algorithm Performances are predictable, once the sampling time is set, the proposed approach can be used in a real-time context.

6. Conclusions

The paper has proposed a linear programming algorithm to compute the globally optimal minimum-time control for a rest-to-rest constrained transitions of a flexible joint. A comparison with an inversion-based feed-forward control has confirmed the effectiveness of the new approach. Moreover, the novel approach applies to any stable linear plant, so that it is foreseeable an extension of the technique to the more challenging cases of systems with unstable zero-dynamics like, for example, flexible links [14].

Appendix A. Proof of Theorem 1

The following lemma will be used in the proof.

Lemma 1. *Consider system (17) and be the pair* $(u(k), y(k)) \in \mathscr{B}_{\mathscr{A}}$. *If*

$$y(i+N) = y_f \quad \text{for } i = 0, \dots, n-1,$$

$$u(i+N) = \frac{y_f}{H(1)} \quad \text{for } i \geqslant 0,$$

then

$$y(i) = y_f \quad \forall i \geqslant N. \tag{A.1}$$

Proof of Lemma. Consider the input–output pair $(u_2(k), y_2(k)) = (u(k) - \frac{y_f}{H(0)}, y(k) - y_f)$. Since $u_2(k) = 0\ \forall k \geqslant N$, therefore, for $k \geqslant N$, $y_2(k)$ satisfies the following difference equation:

$$\begin{cases} a_n y_2(k+n) = -a_{n-1} y(k+n-1) - a_{n-2} y_2(k+n-2) - \cdots - a_0 y_2(k), \\ y_2(N) = y_2(N+1) = \cdots = y_2(N+n-1) = 0, \end{cases}$$

which has solution $y_2(k) = 0 \quad \forall k \geqslant N$. Consequently, (A.1) follows. □

Proof of Theorem. Define a continuous function $l(t)$ which has the following properties:

$$\begin{cases} l(t) = 0 \quad \text{if } t \leqslant 0, \\ l(t) = \frac{y_f}{H(1)} \quad \text{if } t \geqslant 1, \\ 0 \leqslant l(t) \leqslant \frac{y_f}{H(1)} \quad \forall t \in [0,1]. \end{cases}$$

Impose $u_N(k) = l(\frac{k}{N})$ and let $U_N(z)$ be the corresponding Z-transform. Moreover, be $Y_N(z) = U_N(z)H(z)$ and $y_N(k) = \mathscr{Z}^{-1}\{Y_N(z)\}$.

First of all it is proved that

$$\lim_{N \to +\infty} \|H(1)\, u_N(k) - y_N(k)\|_\infty = 0. \tag{A.2}$$

Indeed,

$$H(1)U_N(z) - Y_N(z) = H(1)U_N(z) - H(z)U_N(z) = (H(1) - H(z))U_N(z).$$

Being $H(1) - H(z)|_{z=1} = 0$, function $H(1) - H(z)$ has a zero in $z = 1$. Hence, $H(1) - H(z) = (z-1)H'(z)$, where $H'(z)$ has the same poles as $H(z)$. Therefore $(H(1) - H(z))U_N(z) = H'(z)(z-1)U_N(z)$ and

$$\lim_{N \to +\infty} \|H(1)\, u_N(k) - y_N(k)\|_\infty \leqslant \lim_{N \to \infty} \|\mathscr{Z}^{-1}\{H'(z)\}\|_2 \|u_N(k+1) - u(k)\|_\infty = 0,$$

in fact

$$\lim_{N \to +\infty} \|u_N(k+1) - u(k)\|_\infty = 0$$

because function $l(t)$ is uniformly continuous and $\|\mathscr{Z}^{-1}\{H'(z)\}\|_2$ is finite because $H'(z)$ is stable.

Eq. (A.2) shows that as N approaches infinity, the output $y_N(k)$ becomes equal to input $u_N(k)$ multiplied by the static gain $H(1)$ and, for $k \geqslant N$, the difference $y_N(k) - y_f$ tends to zero. In the following a correcting term $\bar{y}_N(k)$ is introduced such that $y_N(k) + \bar{y}_N(k) = y_f\ \forall k \geqslant N$. Define the error vector $\mathbf{e}_N := (e_{N,0}, e_{N,1}, \dots, e_{N,n-1})^T \in \mathbb{R}^n$ as

$$e_{N,i} = y_N(N+i) - y_f, \quad i = 0, \dots, n-1,$$

let $\mathbf{M} \in \mathbb{R}^{n \times N} = (m_{i,j})$ be such that

$$m_{i,j} = h(j-i), \quad i = 1, \dots, n \quad \text{and} \quad j = 1, \dots, N,$$

where $h(k) = \mathscr{Z}^{-1}\{H(z)\}$ denotes the system impulse response. Set $\bar{\mathbf{u}}_N = (\bar{u}_{N,0}, \bar{u}_{N,1}, \dots, \bar{u}_{N,n-1})^T$ as

$$\bar{\mathbf{u}}_N = -\mathbf{M}^+ \mathbf{e}_N,$$

where $\mathbf{M}^+ = \mathbf{M}^t (\mathbf{M}^t \mathbf{M})^{-1}$ is the pseudo-inverse of $\mathbf{M}$.

Define the correcting input vector $\bar{u}_N$ as

$$\begin{cases} \bar{u}_N(N+k) = \mathbf{u}_{N,k} \quad \text{if } 0 \leqslant k < n-1, \\ 0 \quad \text{otherwise} \end{cases}$$

and let $\bar{y}_N(k)$ be the corresponding output. Consider as input $u_N(k) + \bar{u}_N(k)$, the corresponding output is $y_N(k) + \bar{y}_n(k)$. The following conditions are satisfied:

$$y_N(k) + \bar{y}_N(k) = y_f \quad \forall k \geqslant N, \tag{A.3}$$

$$\lim_{N \to +\infty} \|\bar{u}_N(k)\|_\infty = 0, \tag{A.4}$$

$$\lim_{N \to +\infty} \|\bar{y}_N(k)\|_\infty = 0. \tag{A.5}$$

If fact (A.3) follows from the fact that

$$y_N(N+k) + \bar{y}(N+k) = y_f + e_N(k) - e_N(k) = y_f, \quad k = 0, \dots, n-1$$

and $y_N(k) + \bar{y}_N(k) = y_f\ \forall k \geqslant N$ as a consequence of Lemma 1. Conditions (A.4) and (A.5) follow from the following inequalities:

$$\lim_{N \to +\infty} \|\bar{u}_N(k)\|_\infty \leqslant \|\mathbf{M}^+\|_2 \lim_{N \to +\infty} \|e_n\|_\infty = 0,$$

$$\lim_{N \to +\infty} \|\bar{y}_N(k)\|_\infty \leqslant \|h(k)\|_2 \|\mathbf{M}^+\|_2 \lim_{N \to +\infty} \|e_n\|_\infty = 0,$$

being $\lim_{N \to \infty} \|e_n\|_\infty = 0$ by (A.2).

Therefore

$$\lim_{N\to\infty} \max\left\{u_N(k)+\bar{u}_N(k)-\frac{y_f}{H(1)}, -u_N(k)-\bar{u}_N(k), y_N(k)+\bar{y}_N(k) -y_f, -y_N(k)-\bar{y}_N(k)\right\}=0$$

and, because of (24), for N sufficiently large the following property holds:

$$\max\{u_N(k)+\bar{u}_N(k)-u_c^+, -u_N(k)-\bar{u}_N(k)-u_c^-, y_N(k)+\bar{y}_N(k)-y_c^+, -y_N(k)-\bar{y}_N(k)-y_c^-\}$$

therefore all properties (19)–(22) are verified. In fact (19) is verified by construction, (21) comes from (A.3) and (20), (22) follow from (A.6). □

Appendix B. Proof of Proposition 2

For any $k\in\mathbb{Z}$ and $\tau\in[0,1]$, set

$$e(\tau)=y(kT+\tau T)-[\tau y((k+1)T)+(1-\tau)y(kT)] \tag{B.1}$$

and note that $e(0)=e(1)=0$. Since $y(kT+\tau T)=\mathbf{C}e^{\mathbf{A}\tau T}x(kT)+\mathbf{C}\int_0^{\tau T}e^{\mathbf{A}h}\mathbf{B}u(kT)\,dh$ Eq. (B.1) becomes

$$e(\tau)=\mathbf{C}(e^{\mathbf{A}\tau T}-I-\tau(e^{\mathbf{A}T}-I))x(kT) +\mathbf{C}\left(\int_0^{\tau T}e^{\mathbf{A}h}\,dh-\tau\int_0^{T}e^{\mathbf{A}h}\,dh\right)\mathbf{B}u(kT). \tag{B.2}$$

It is known that

$$\int_0^x e^{\mathbf{A}h}\,dh=(e^{\mathbf{A}x}-I)\mathbf{A}^{-1};$$

therefore (B.2) can be rewritten as follows:

$$e(\tau)=\mathbf{C}(e^{\mathbf{A}\tau T}-I-\tau(e^{\mathbf{A}T}-I))(x(kT)+\mathbf{A}^{-1}\mathbf{B}u(kT)). \tag{B.3}$$

Define $z(\tau)=\mathbf{C}(e^{\mathbf{A}\tau T}-I-\tau(e^{\mathbf{A}T}-I))$. It is easily verifed that $z(0)=0$ and $\frac{dz}{d\tau}(0)=0$. Consequently $z(\tau)$ can be expanded as follows:

$$z(\tau)=\mathbf{C}\sum_{i=2}^{+\infty}\frac{\mathbf{A}^iT^i\tau^i}{i!}, \tag{B.4}$$

i.e. the two first element of the series are missing. Eq. (B.4) can be manipulated leading to

$$z(\tau)\leqslant\sum_{i=2}^{+\infty}\frac{\|\mathbf{C}\mathbf{A}^iT^i\|\tau^i}{i!}\leqslant\sum_{i=2}^{l}\frac{\|\mathbf{C}\mathbf{A}^iT^i\|}{i!}+\|\mathbf{C}\|\sum_{i=l+1}^{+\infty}\frac{\|\mathbf{A}T\|^i}{i!} =\mathbf{C}(e^{\|\mathbf{A}\|T}-I-\|\mathbf{A}\|T)-\sum_{i=2}^{l}(\|\mathbf{C}\|\|\mathbf{A}\|^i-\|\mathbf{C}\mathbf{A}^i\|)\frac{T^i}{i!}. \tag{B.5}$$

Finally, substituting (B.5) in (B.3) and using the fact that $\max_{t\in\mathbb{R}}\{y(t)-y_c^+,\ y_c^--y(t)\}\leqslant\max_{t\in\mathbb{R}}|e(t)|$ we obtain the thesis. □

Appendix C. Proof of Proposition 3

Define $\bar{y}=y-y_f$ and $\bar{u}=u-\frac{y_f}{H(0)}$, then the following differential equation is satisfied $\forall t\geqslant t_0$

$$D^n\bar{y}(t)+a_{n-1}D^{n-1}\bar{y}(t)+\cdots+a_0\bar{y}(t)=0. \tag{C.1}$$

Indicate with ρ_i, $i=1,\ldots,l$ the multiplicities respectively associated to any root p_i, then, $\forall t\geqslant t_0$ the solution of (C.1) can be expressed in the following form:

$$y(t)=\sum_{i=1,\ldots,l}\ \sum_{j=0,\ldots,\rho_i-1}c_{i,j}\cdot\frac{(t-t_0)(t-t_0-T)\cdots(t-t_0-(j-1)T)}{T^j(j-1)!}e^{p_i(t-t_0-jT)}, \tag{C.2}$$

where $C_{i,j}$ are suitable constants. Due to (C.2), Eq. (30) can be written as follows:

$$0=\mathbf{V}\mathbf{C}, \tag{C.3}$$

where $\mathbf{V}=[\mathbf{V}_1,\mathbf{V}_2,\ldots,\mathbf{V}_l]$ and

$$\mathbf{V}_i=\begin{bmatrix}1 & 0 & 0 & \ldots & 0\\ e^{Tp_i} & 1 & 0 & \ldots & 0\\ \vdots & \vdots & \vdots & \vdots & \\ e^{(\rho_i-1)Tp_i} & (\rho_i-1)e^{(\rho_i-1)Tp_1} & \frac{(\rho_i-2)(\rho_i-1)}{2}e^{(\rho_i-1)Tp_i} & \ldots & 1\end{bmatrix},$$

$$\mathbf{C}=\left(c_{1,0},\ c_{1,1},\ \ldots,\ c_{1,\rho_1-1},\ c_{2,0},\ \ldots,\ c_{l,\rho_l-1}\right)^T.$$

$\mathbf{V}$ is the *generalized Vandermonde matrix* and, as stated in [9], $det(\mathbf{V})=\prod_{1\leqslant i<j\leqslant l}(e^{p_iT}-e^{p_jT})^{\rho_i\rho_j}$. Because of (31), $det\mathbf{V}\neq0$, so that from (C.3) it follows that $\mathbf{C}=0$, and therefore $y(t)=0\ \forall t\geqslant t_0$. □

References

[1] Albu-Schäffer A, Ott C, Hirzinger G. A unified passivity-based control framework for position, torque and impedance control of flexible joint robots. Int J Robot Res 2007;26(1):23–39.

[2] Bicchi A, Tonietti G. Fast and "soft-arm" tactics. IEEE Robot Autom Mag 2004;11(2):22–33.

[3] Dahl O. Path constrained motion optimization for rigid and flexible joint robots. In: Proceedings of IEEE international conference on robotics and automation, 1993, vol.2, May 1993. p. 223–9.

[4] GNU Foundation. Gplk, gnu linear programming kit. Available at: <http://www.gnu.org/software/glpk/>.

[5] Bashein G. A simplex algorithm for on-line computation of time optimal controls. IEEE Trans Autom Control 1971.

[6] Palli G, Melchiorri C, De Luca A. On the feedback linearization of robots with variable joint stiffness. In: 2008 IEEE international conference on robotics and automation, 2008. p. 1753–9.

[7] Guarino Lo Bianco C, Piazzi A. A servo control system design using dynamic inversion. Control Eng Practice 2002;10(8):847–55.

[8] Chiasson J. Modeling and high-performance control of electric machines. Wiley Interscience; 2005.

[9] Dan Kalman. The generalized vandermonde matrix. Math Mag 1984;57(1):15–21.

[10] Kim MH, Engell S. Speed-up of linear programming for time-optimal control. In: Proceedings of the 1994 american control conference, ACC94, 1994. p. 2667–70.

[11] Scott M. Time/fuel optimal control of constrained linear discrete systems. Automatica 1986.

[12] Giorgietti N. Gplkmex, a matlab mex interface for the gplk library. Available at: <http://glpkmex.sourceforge.net/>.

[13] Karmarkar N. A new polynomial-time algorithm for linear programming, Report. AT&T Bell Laboratories, 1984.

[14] Piazzi A, Visioli A. End-point control of flexible link via optimal dynamic inversion. In: Proceedings of the 2001 IEEE/ASME international conference on advanced intelligent mechatronics, Como, Italy, July 2001. p. 936–41.

[15] Piazzi A, Visioli A. Optimal noncausal set-point regulation of scalar systems. Automatica 2001;37(1):121–7.

[16] Shamir R. The efficiency of the simplex method: a survey. Manage Sci 1987;33(3):301–34.

[17] Kim S, Choi D, Ha I. A comparison principle for state-constrained differential inequalities and its application to time-optimal control. IEEE Trans Autom Control 2005.

[18] Ozgoli S, Taghirad HD. A survey on the control of flexible joint robots. Asian J Control 2006;8(4):1–15.

[19] Zadeh LA. On optimal control and linear programming. IRE Trans Autom Control 1962:45–6.